Int. J. Nano Dimens., 7 (3): 254-262, Summer 2016

ORIGINAL ARTICLE

Acetone sensing properties of hierarchical WO_3 core-shell microspheres in comparison with commercial nanoparticles

Mostafa Esmaeili[1]; Gholamreza Kiani[1,]; Farhad Shahriari Nogorani[2]; Saeed Boroomand[2]*

[1]*School of Engineering Emerging Technologies, University of Tabriz, Tabriz, Iran*
[2]*Department of Materials Science and Engineering, Shiraz University of Technology, Shiraz, Iran*

Received 19 December 2015; revised 25 April 2016; accepted 20 May 2016; available online 18 June 2016

Abstract

In this work, hierarchical WO_3 core-shell microspheres were synthesized via a facile template-free precipitation method. Gas sensing properties of the synthesized powder to acetone and some other volatile organic compounds were comparatively investigated with commercial WO_3 nanoparticles. The synthesized and commercial powders were characterized by X-ray diffraction, scanning electron microscopy, particle size distribution analysis, Brunauer–Emmett–Teller and Barrette-Joyner-Halenda techniques. Gas sensors were fabricated by deposition of powders between/on interdigitated electrodes via sedimentation approach. The results show that both sensors are sufficiently sensitive to detect 1.8 ppm of acetone; diabetes diagnosis threshold in human exhaled breath. Indeed, the hierarchical based one is highly sensitive and more selective to acetone.

Keywords: *Acetone; Core-shell microspheres; Diabetes; Gas sensor; Nanoparticles; WO_3.*

How to cite this article

Esmaeili M, Kiani G R, Shahriari Nogorani F, Boroomand S. Acetone sensing properties of hierarchical WO3 core-shell microspheres in comparison with commercial nanoparticles. Int. J. Nano Dimens., 2016; 7(3): 254-262.,DOI: 10.7508/ijnd.2016.03.009.

INTRODUCTION

Metal oxide semiconductor gas sensors have drawn attentions of many researches in the past few years due to their high sensitivity to various gases, fast response and miniaturization potentiality. Tungsten oxide as an n-type wide bandgap metal oxide semiconductor that has a fame for electrochromism [1, 2] and photocatalysis [3, 4] is less studied for this purpose, while this functional material shows great sensitivity to NO_2 [5-7] and some volatile organic compounds [8-11] including acetone [12-14]. Amongst VOCs, acetone has been introduced as diabetes biomarker in human exhaled breath [15-17] assuming that nutritional effects such as postprandium and diurnal fluctuations are neglected [18]. In view of a report in the literature, concentration of acetone in a diabetic patient breath is considered to be higher than 1.8 ppm [17]; however, quantification of the relationship between exhaled VOCs and different aspects of diabetes still needs further investigations [19].

* Corresponding Author Email: g.kiani@tabrizu.ac.ir

In order to enhance gas sensing performance of metal oxide semiconductors, nanostructures with increased surface area which provide complete electron depletion are desirable [20,21]. With the advent of nanotechnology, an assortment of metal oxide nanostructures including nanoparticles [13], nanowires [6], nanoribbons [22], nanobelts [23], nanorods [24], nanoplates [7], nanosheets [25], nanofibers [10], nanotubes [14], nanocubes [11] have been explored for this aim. Nanoparticles are the most common form of nanostructures which are employed in this area of study. Their major drawback is that aggregation between particles is inevitable when they are consolidated into sensing films [26] as van der Waals attraction is inversely proportional to the particle size. Under this agglomerated configuration only particles near surface region participate in gas sensing reaction and inner parts remain inactive; therefore a great response cannot be accomplished [27].

Hierarchical structures with well-defined mesoporous architecture can be the clue to

overcome the abovementioned issue because they provide porosity for effective gas diffusion without sacrificing a high surface area [28]. In this study, hierarchical WO_3 core-shell microspheres were synthesize through proposed methodology by Zhang and co-workers [4] and gas sensing properties of the synthesized powder to acetone and some other VOCs were investigated and compared with commercial WO_3 nanoparticles.

EXPERIMENT

Samples preparation

WO_3 nanoparticles were purchased from US Research Nanomaterials, Inc (product code: US3540). For preparation of hierarchical WO_3 structures, all chemicals were used without further purification. In a typical procedure, 10 mL $CaCl_2$ solution (0.5 M), 3 mL citric acid solution (10 g/L), and 27 mL distilled water were mixed in a beaker under magnetic stirring for 5 minutes. Then, 10 mL Na_2WO_4 solution (0.5 M) was slowly added under vigorous stirring. The initial pH value of the mixture was adjusted to 12 using NaOH (2 M) solution. After continuous vigorous stirring for 5 minutes, the mixture was sealed and kept at room temperature for 24 hours. Thereafter, the resulting white precipitate was collected, washed with distilled water and ethanol, and dried in air. To prepare hierarchical WO_3 core-shell microspheres, the obtained powder was soaked in HNO_3 (8 M) for 24 hours at room temperature, followed by calcination at 480 °C for 2 hours, resulting in a yellow powder.

Samples characterization

The samples morphology was examined using scanning electron microscopy (TESCAN, MIRA3 & VEGA3 LM). BET analysis in tandem with BJH method (Microtrac, Belsorp-Mini II) was carried out to determine specific surface area and pore size distribution of the samples. To ascertain particle size distribution of the commercial nanoparticles, this analysis were done based on dynamic light scattering methodology (Microtrac, Nanotrac Wave). Crystallographic information for the specimens was obtained using powder X-ray diffraction (Siemens D5000).

Interdigitated electrodes

13mm*15mm electrodes were purchased from Electronic Design Center of Case Western Reserve University. These electrodes consist of interdigitated platinum lines (250 µm width and spacing) and platinum resistance temperature detector on one side of an alumina substrate and a platinum heater on the other side. Contacts and heaters on the base of Pt have been stated as the most stable material at relatively high temperatures [29].

Sensors fabrication

To make gas sensors, 0.025 g of each WO_3 powders were added to 5 mL acetone in 10 mL beakers and ultrasonicated for 10 minutes. Afterwards interdigitated electrodes were placed at the bottom of beakers. Beakers were kept in still positions until the acetone fully vaporized and sediments deposited between/on interdigitated electrodes. Then the substrates were dried at 75 °C for one hour and finally the bonding pads were cleaned. In this step acetone was employed as suspension medium because of its high evaporation rate.

Test apparatus

Gas sensing experiments were performed in air vicinity in a 16 L volume glovebox-like homemade setup (Fig. 1). The examined analytes were some VOCs including acetone, ethanol, methanol, ammonia, xylene and toluene. The box was contaminated by injecting predetermined volumes of the liquid chemicals which were evaporated in the chamber. The chamber air was homogenized continuously by the mild agitation of a small fan. Vacuum pump was employed to expel gas from the chamber. Data acquisition unit records electrical resistance behaviour of the as-fabricated sensors under gas contamination.

RESULTS AND DISCUSSION

Morphological and structural characteristics

X-ray diffraction patterns: The XRD patterns of WO_3 powders are shown in Fig. 2. They indicate presence of the characteristic diffraction peaks corresponding to WO_3 for both commercial and synthesized powders. Diffraction peaks related to commercial nanoparticles and hierarchical microspheres are shown in Fig. 2. a and Fig. 2. b respectively.

Particle size distribution analysis: Mean size distribution of the as-received commercial WO_3 nanoparticles are depicted in Fig. 3. As can be seen, particles are in the range of 35 nm to 90 nm.

Scanning electron microscopy images: Fig. 4a shows typical SEM images of WO_3 nanoparticles. Careful observation of particles (Fig. 4b) indicates

tolerable good agreement with PSDA results. Uniformly-sized hierarchical WO_3 core-shell microspheres with a diameter of 5-10 µm can be clearly observed in Fig. 5a. High magnification SEM image of a typical WO_3 microsphere surface reveals roughness and porosity of the structure (Fig. 5b). Some broken spheres can be distinctly seen in Fig. 5c implying that the WO_3 microspheres have a solid interior. Fig. 5d which is a zoomed-in area of a broken sphere surface in Fig. 5c confirms that the microspheres are really composed of a core part.

Brunauer-Emmett-Teller and Barrett-Joyner-Halenda analysis: Figs. 6-7 show the N_2 adsorption-desorption isotherm of the WO_3 microspheres and nanoparticles. The BET specific area for the microspheres and nanoparticles is 13.68 m^2/g and 15.08 m^2/g respectively. In addition, the pore size distribution diagrams (Figs. 8-9) which were obtained based on BJH method indicates that the pore density in both cases is in the mesoporous region. The total pore volume for the microspheres and nanoparticles is 0.13 cm^3/g and 0.08 cm^3/g correspondingly.

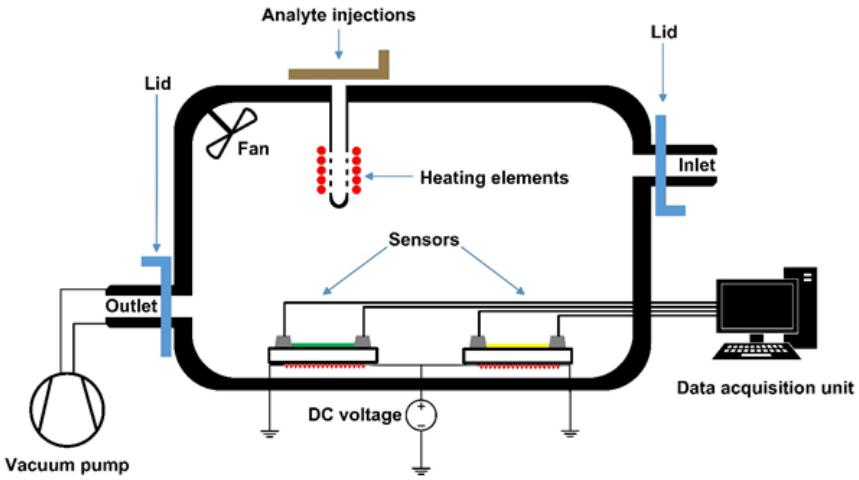

Fig. 1: The schematics of the experimental setup.

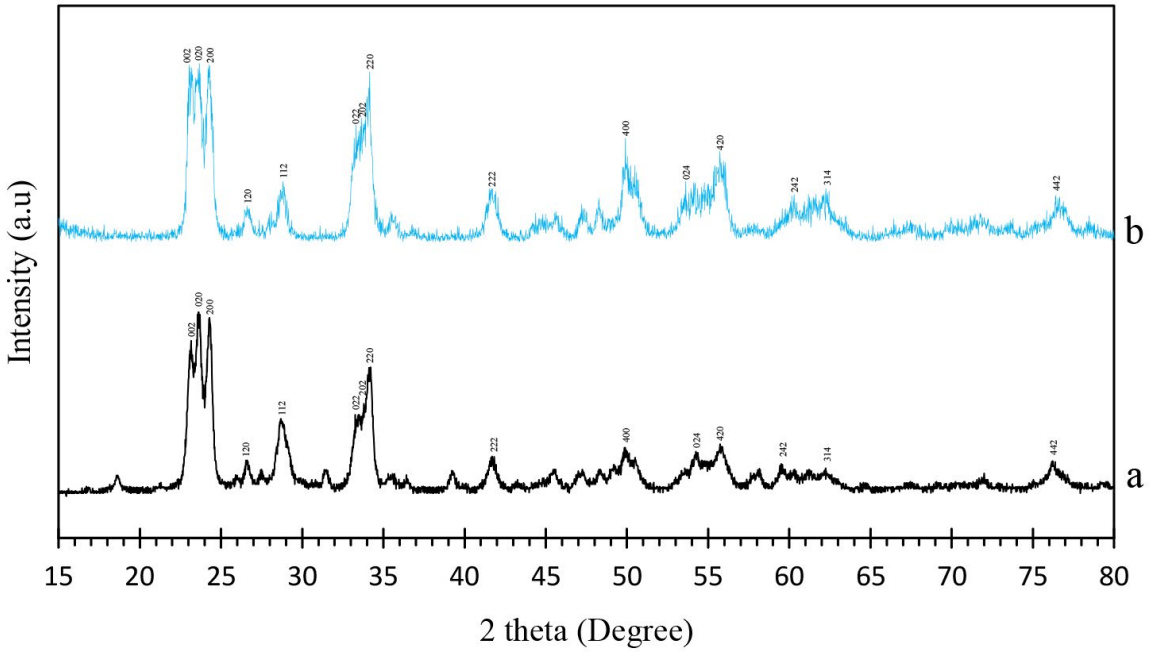

Fig. 2: XRD patterns of the (a) hierarchical WO_3 microspheres, (b) commercial WO_3 nanoparticles.

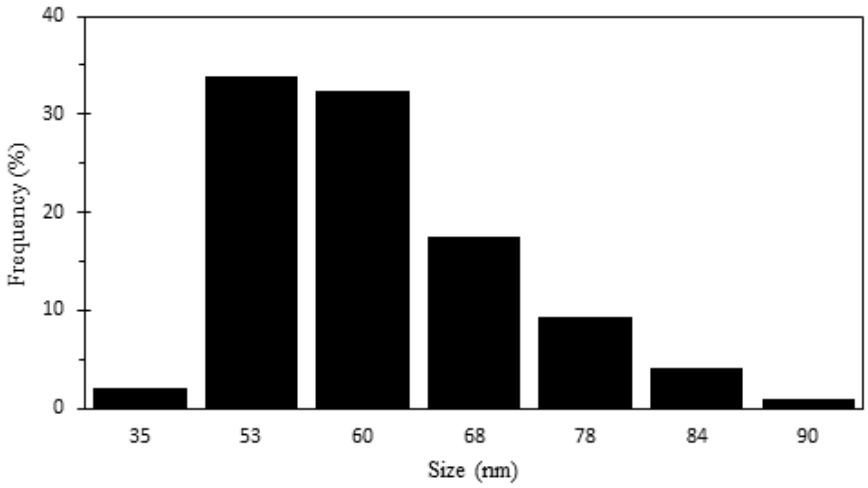

Fig. 3: Particle size distribution of the commercial WO_3 nanoparticles.

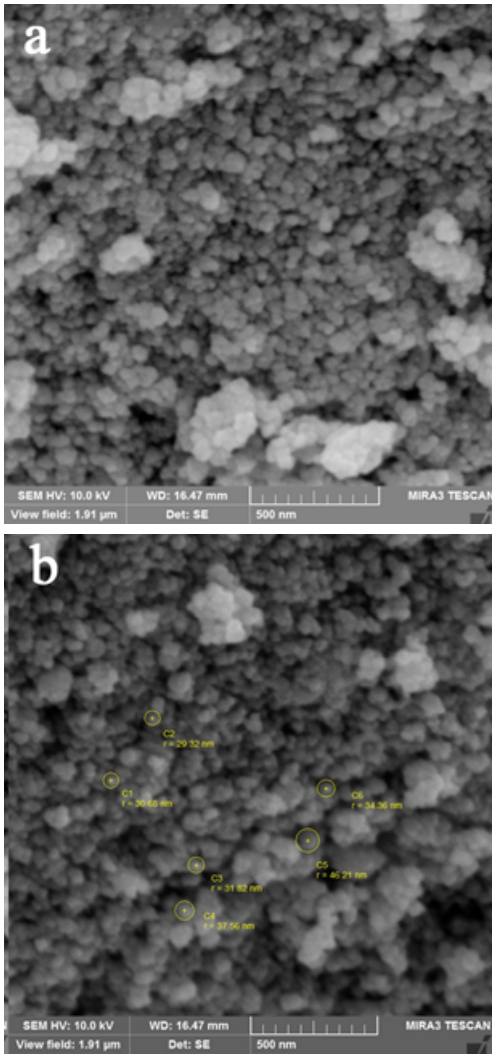

Fig. 4: SEM images of the commercial WO_3 nanoparticles (a) without (b) with indicators showing some typical particles size.

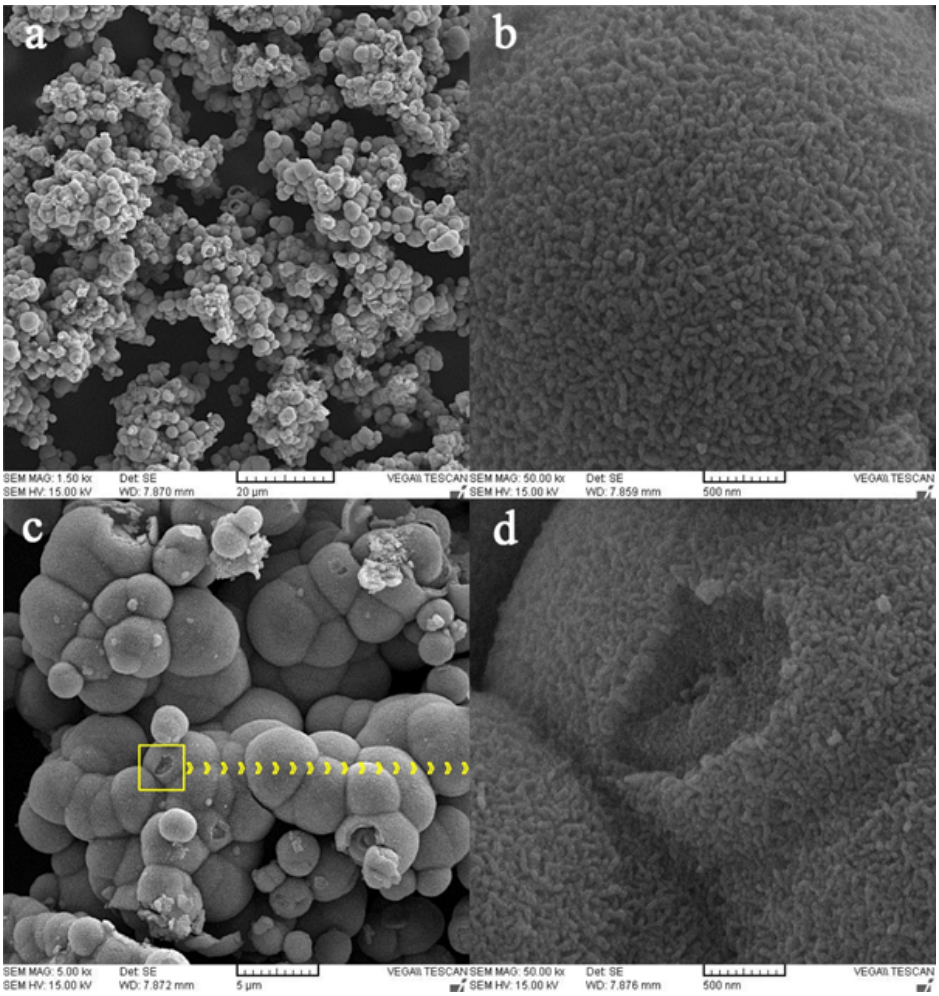

Fig. 5: (a) Low magnification SEM image of the hierarchical WO_3 core-shell microspheres; (b) High magnification SEM image of a typical microsphere surface; (c) SEM image of some broken spheres; (d) Zoomed-in surface area of a broken sphere.

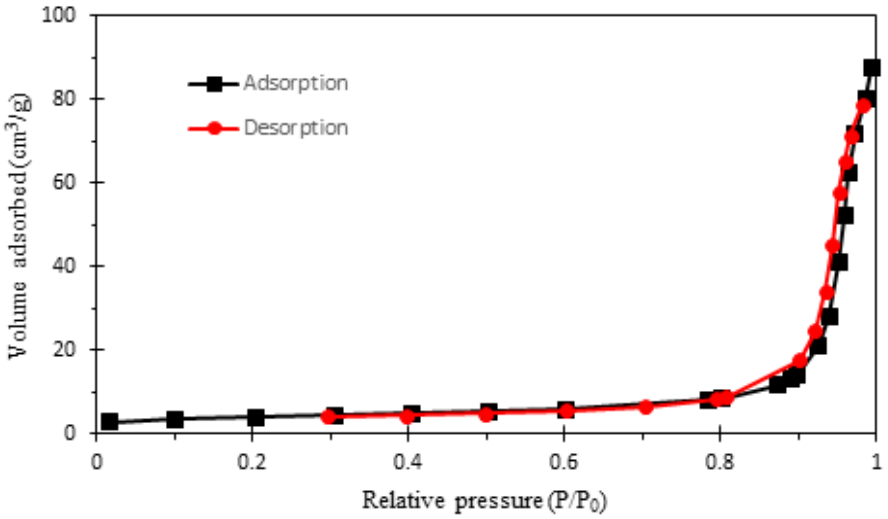

Fig. 6: Nitrogen adsorption and desorption isotherms of the hierarchical WO_3 microspheres.

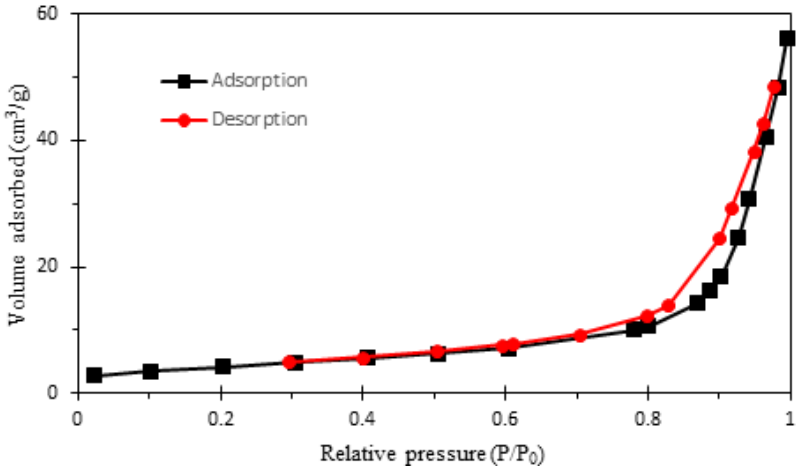

Fig. 7: Nitrogen adsorption and desorption isotherms of the commercial WO_3 nanoparticles.

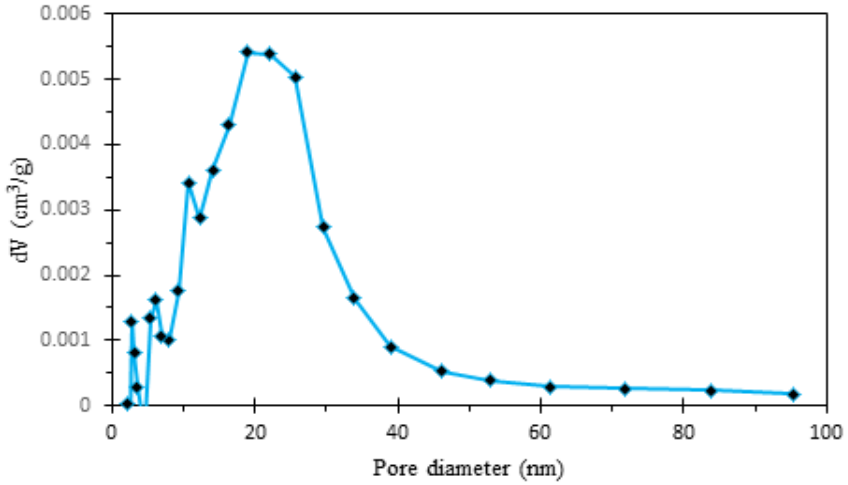

Fig. 8: Pore size distribution curve of the hierarchical WO_3 microspheres.

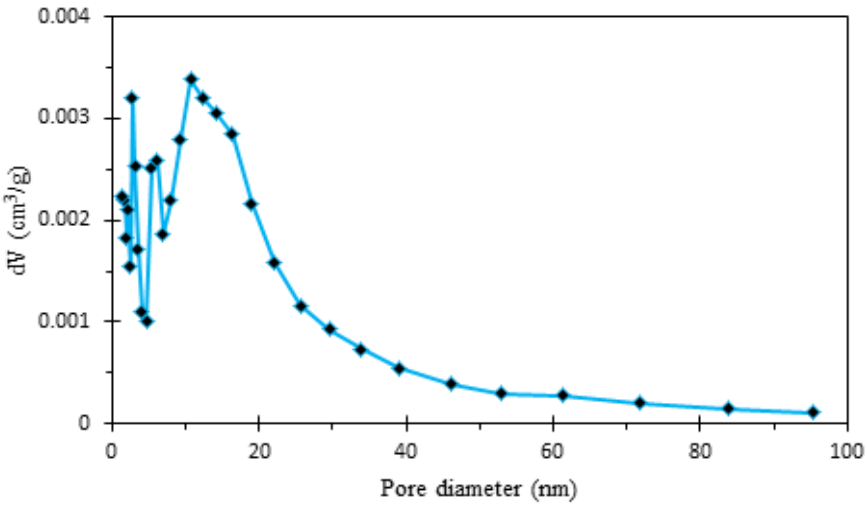

Fig. 9: Pore size distribution curve of the commercial WO_3 nanoparticles.

Gas sensing properties

In order to obtain optimum working temperatures of the as-fabricated sensors, an intermittent sensitivity measurement of 50 ppm of acetone with 50 °C steps from 50 °C to 350 °C was performed (Fig. 10). The results point out that the best performance of the hierarchical structure based sensor is at 300 °C and the nanoparticle based one at 350 °C. Sensitivity of both sensors to 10 ppm of some VOCs at 300 °C is depicted in a bar chart (Fig. 11) which shows the highest sensitivity to acetone for either sensor. Evidently, microsphere based sensor responds to acetone more selectively. Figs. 12-13 show response time of the sensors to 1.8, 5, 10, 50 ppm of acetone at their optimum working temperatures. As can be seen in these figures, both sensors are capable of detecting diabetes diagnosis threshold rapidly and adequately. These figures also illustrate that the sensitivity of the microsphere based sensor to different concentrations of acetone in spite of lowered working temperature is superior to the nanoparticle based one.

The better response of the hierarchical structure can be attributed to its less agglomerative configuration. From this improved response, it can also be inferred that apart from surface area, porosity and roughness of the structure play crucial roles in enhancing gas sensing properties of the device.

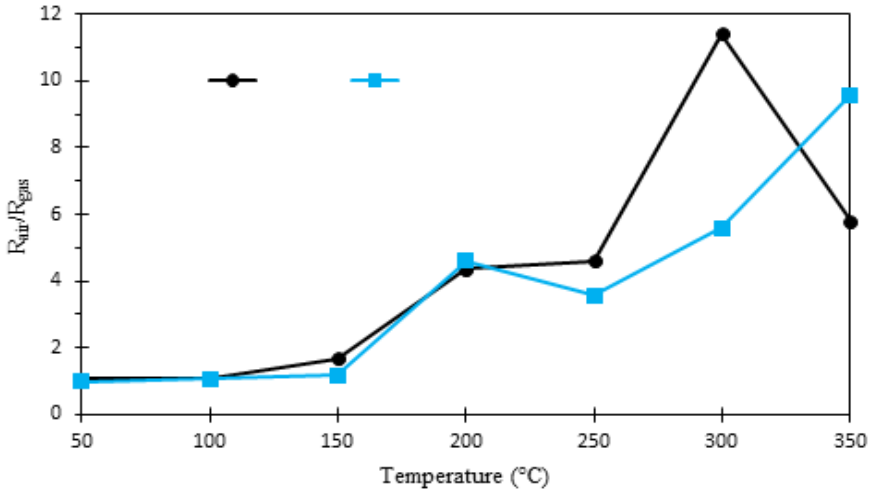

Fig. 10: Sensitivity of the WO_3 microsphere and nanoparticle based sensors to 50 ppm of acetone at different working temperatures.

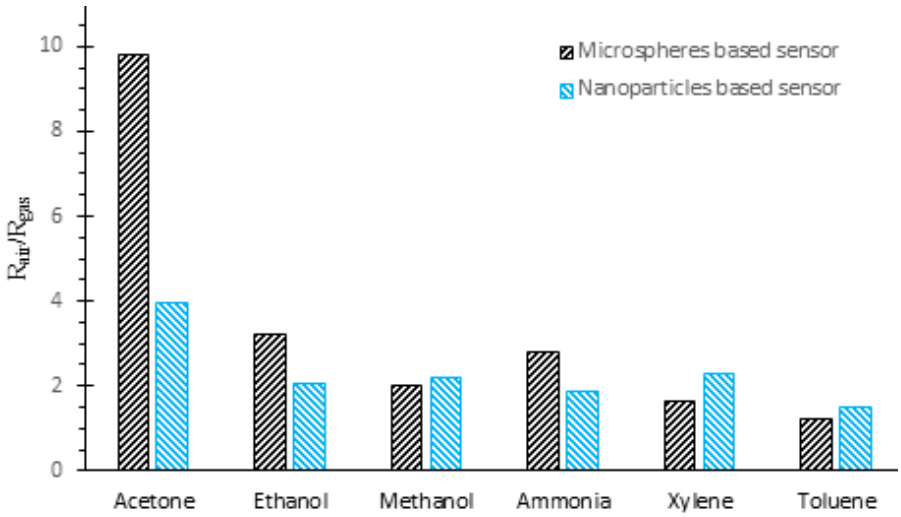

Fig. 11: Sensitivity of the WO_3 microsphere and nanoparticle based sensors to 10 ppm of some VOCs at 300°C.

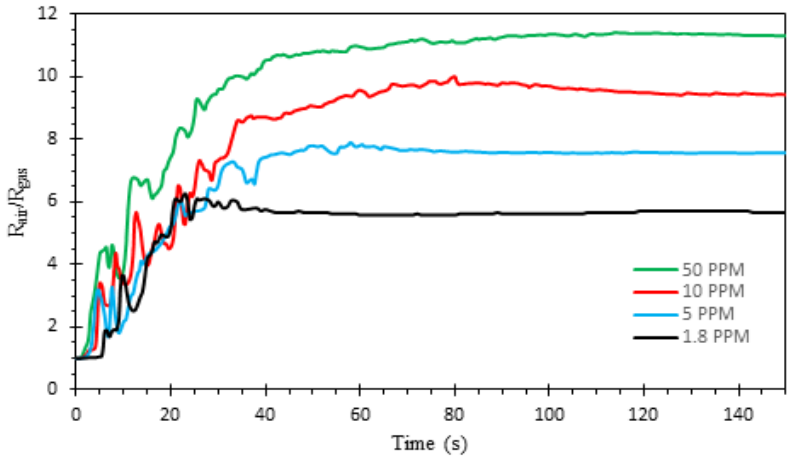

Fig. 12: Gas response of the WO_3 microsphere based sensor to different concentrations of acetone at 300 °C.

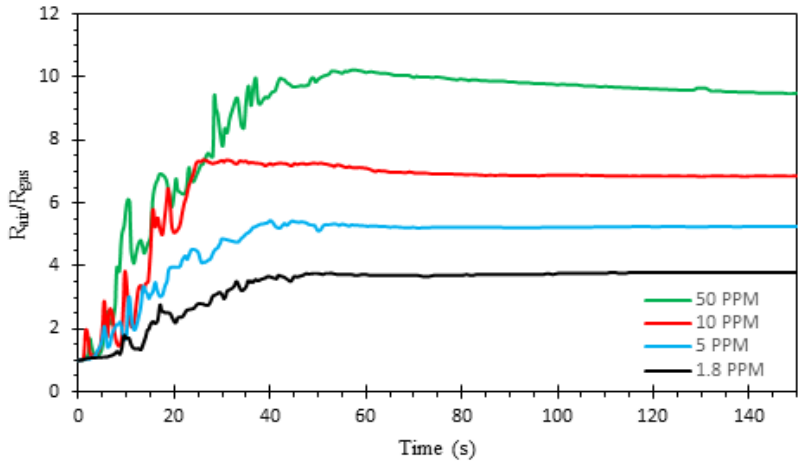

Fig. 13: Gas response of the WO_3 nanoparticle based sensor to different concentrations of acetone at 350 °C.

Briefly, when WO_3 as an n-type semiconductor whose major charge carriers are electrons is exposed to atmosphere, the air which contains oxygen as an oxidizing gas adsorbs electrons from the surface of the material to produce negatively charged chemisorbed oxygen species such as O_2^- and O^-. The process can be described as follows:

$$(1)\ O_2 + e^- \rightarrow O_2^-;$$

$$(2)\ O_2^- + e^- \rightarrow 2O^-;$$

When a fraction of acetone as a reducing gas is injected to the surrounding air of the sensing film, it reacts with chemisorbed oxygen species:

$$(3)\ CH_3COCH_3 + O_2^- \rightarrow CH_3C^+O + CH_3O^- + 2e^-;$$

$$(4)\ CH_3C^+O \rightarrow C^+H_3 + CO;$$

$$(5)\ CO + O^{2-} \rightarrow CO_2 + 2e^-.$$

Thereby a quantity of electrons proportional to the concentration of target gas are released to the conduction band of the material, band bending occurs and the electrical conductance of the semiconductor increases.

CONCLUSION

In this work we presented fabrication of a real-time highly sensitive and fairly selective acetone sensor for detection of diabetes diagnosis threshold in human breath using hierarchical WO_3 core-shell microsphere structures.

Comparing electrical resistance behaviour of the WO_3 nanoparticles and microspheres at different temperatures under acetone contamination demonstrated that except for specific surface area, porosity and roughness of the structure are of

great importance to reduce working temperature and enhance sensitivity.

CONFLICT OF INTEREST

The authors declare that there is no conflict of interests regarding the publication of this manuscript.

REFERENCES

[1] Granqvist C. G., (1995), Handbook of inorganic electrochromic materials. *Elsevier*.

[2] Deb S. K., (2008), Opportunities and challenges in science and technology of WO_3 for electrochromic and related applications. *Sol. Energ. Mat. Sol. C.* 92: 245-258.

[3] Zhang H., Chen G., Bahnemann D. W., (2009), Photoelectrocatalytic materials for environmental applications. *J. Mater. Chem.* 19: 5089-5121.

[4] Zhang L., Tang X., Lu Z., Wang Z., Li L., Xiao Y., (2011), Facile synthesis and photocatalytic activity of hierarchical WO_3 core–shell microspheres. *Appl. Surf. Sci.* 258: 1719-1724.

[5] Afzal A., Cioffi N., Sabbatini L., Torsi L., (2012), NO_x sensors based on semiconducting metal oxide nanostructures: Progress and perspectives. *Sensor. Actuat. B: Chem.* 171: 25-42.

[6] Ponzoni A., Comini E., Sberveglieri G., Zhou, J., Deng S. Z., Xu N. S., (2006), Ultrasensitive and highly selective gas sensors using three-dimensional tungsten oxide nanowire networks. *Appl. Phys. Lett.* 88: 203101.

[7] Kim S. J., Hwang I. S., Choi J. K., Lee J. H., (2011), Gas sensing characteristics of WO_3 nanoplates prepared by acidification method. *Thin Solid Films.* 519: 2020-2024.

[8] Li X. L., Lou T. J., Sun X. M., Li Y. D., (2004), Highly sensitive WO_3 hollow-sphere gas sensors. *Inorg. Chem.* 43: 5442-5449.

[9] Kanda K., Maekawa T., (2005), Development of a WO_3 thick-film-based sensor for the detection of VOC. *Sensor. Actuat. B: Chem.* 108: 97-101.

[10] Shin J., Choi S. J., Youn D. Y., Kim I. D., (2012), Exhaled VOCs sensing properties of WO_3 nanofibers functionalized by Pt and IrO_2 nanoparticles for diagnosis of diabetes and halitosis. *J. Electroceram.* 29: 106-116.

[11] Li X., Zhang G., Cheng F., Guo B., Chen J., (2006), Synthesis, characterization, and gas-sensor application of WO_3 nanocuboids. *J. Electrochem. Soc.* 153: H133-H137.

[12] Choi S. J., Lee I., Jang B. H., Youn D. Y., Ryu W. H., Kim I. D., (2013), Selective diagnosis of diabetes using Pt-functionalized WO_3 hemitube networks as a sensing layer of acetone in exhaled breath. *Anal. Chemi.* 85: 1792-1796.

[13] Wang L., Teleki A., Pratsinis S. E., Gouma, P. I., (2008), Ferroelectric WO_3 nanoparticles for acetone selective detection. *Chem. Mater.* 20: 4794-4796.

[14] Chi X., Liu C., Liu L., Li Y., Wang Z., Bo X., (2014), Tungsten trioxide nanotubes with high sensitive and selective properties to acetone. *Sensor. Actuat. B: Chem.* 194: 33-37.

[15] Nelson N., Lagesson V., Nosratabadi A. R., Ludvigsson J., Tagesson C., (1998), Exhaled isoprene and acetone in newborn infants and in children with diabetes mellitus. *Pediatr. Res.* 44: 363-367.

[16] Greiter M. B., Keck L., Siegmund T., Hoeschen C., Oeh U., Paretzke H. G., (2010), Differences in exhaled gas profiles between patients with type 2 diabetes and healthy controls. *Diabetes Technol. The.* 12: 455-463.

[17] Deng C., Zhang J., Yu X., Zhang W., Zhang X., (2004), Determination of acetone in human breath by gas chromatography–mass spectrometry and solid-phase microextraction with on-fiber derivatization. *J. Chromatogr. B.* 810: 269-275.

[18] Smith D., Spanel P., Davies S., (1999), Trace gases in breath of healthy volunteers when fasting and after a protein-calorie meal: A preliminary study. *J. Appl. Physiol.* 87: 1584-1588.

[19] Smith D., Spanel P., Fryer A. A., Hanna F., Ferns G. A., (2011), Can volatile compounds in exhaled breath be used to monitor control in diabetes mellitus?. *J. Breath Res.* 5: 022001.

[20] Kalantarzadeh K., Fry B., (2007), Nanotechnology-enabled sensors. *Springer Science & Business Media.*

[21] Huang X. J., Choi Y. K., (2007), Chemical sensors based on nanostructured materials. *Sensor. Actuat. B: Chem.* 122: 659-671.

[22] Khiabani P. S., Hosseinmardi A., Marzbanrad E., Ghashghaie S., Zamani C., Raissi B., (2012), NO_2 gas sensor fabrication through AC electrophoretic deposition from electrospun In_2O_3 nanoribbons. Sensor. *Actuat. B: Chem.* 162: 102-107.

[23] Comini E., Faglia G., Sberveglieri G., Pan Z., Wang Z. L., (2002), Stable and highly sensitive gas sensors based on semiconducting oxide nanobelts. *Appl. Phys. Lett.* 81: 1869-1871.

[24] Oh E., Choi H. Y., Jung S. H., Cho S., Kim J. C., Lee K. H., (2009), High-performance NO_2 gas sensor based on ZnO nanorod grown by ultrasonic irradiation. *Sensor. Actuat. B: Chem.* 141: 239-243.

[25] Xu M. H., Cai F. S., Yin J., Yuan Z. H., Bie L. J., (2010), Facile synthesis of highly ethanol-sensitive SnO_2 nanosheets using homogeneous precipitation method. Sensor. *Actuat. B: Chem.* 145: 875-878.

[26] Korotcenkov G., (2008), The role of morphology and crystallographic structure of metal oxides in response of conductometric-type gas sensors. *Mater. Sci. Eng. R.* 61: 1-39.

[27] Korotcenkov G., (2005), Gas response control through structural and chemical modification of metal oxide films: state of the art and approaches. *Sensor. Actuat. B: Chem.* 107: 209-232.

[28] Lee J. H., (2009), Gas sensors using hierarchical and hollow oxide nanostructures: overview. *Sensor. Actuat. B: Chem.* 140: 319-336.

[29] Korotcenkov G., Cho B. K., (2011), Instability of metal oxide-based conductometric gas sensors and approaches to stability improvement (short survey). *Sensor. Actuat. B: Chem.* 156: 527-538.